Lab on a Chip

PAPER

View Article Online
View Journal | View Issue

Cite this: *Lab Chip*, 2017, **17**, 1323

A passive microfluidic system based on step emulsification allows the generation of libraries of nanoliter-sized droplets from microliter droplets of varying and known concentrations of a sample†

W. Postek, T. S. Kaminski and P. Garstecki*

We present a novel geometry of microfluidic channels that allows us to passively generate monodisperse emulsions of hundreds of droplets smaller than 1 nL from collections of larger (*ca.* 0.4 μL) mother droplets. We introduce a new microfluidic module for the generation of droplets *via* passive break-up at a step. The module alleviates a common problem in step emulsification with efficient removal of the droplets from the vicinity of the step. In our solution, the droplets are pushed away from the step by a continuous liquid that bypasses the mother droplets *via* specially engineered bypasses that lead to the step around the main channel. We show that the bypasses tighten the distribution of volume of daughter droplets and eliminate subpopulations of daughter droplets. Clearing away the just produced droplets from the vicinity of the step provides for similar conditions of break-up for every subsequent droplet and, consequently, leads to superior monodispersity of the generated emulsions. Importantly, this function is realized autonomously (passively) in a protocol in which only a sequence of large mother droplets is forced through the module. Our system features the advantage of step emulsification systems in that the volumes of the generated droplets depend very weakly on the rate of flow through the module – an increase in the flow rate by 300% causes only a slight increase of the average diameter of generated droplets by less than 5%. We combined our geometry with a simple T-junction and a simple trap-based microdroplet dilutor to produce a collection of libraries of droplets of gradually changing and known concentrations of a sample. The microfluidic system can be operated with only two syringe pumps set at constant rates of flow during the experiment.

Received 4th January 2017,
Accepted 1st March 2017

DOI: 10.1039/c7lc00014f

rsc.li/loc

Introduction

Here we demonstrate a microfluidic module—*DropChop*—that allows for step emulsification of a series of large droplets without additional equipment designated to push the generated small droplets away from the step. The *DropChop* module passively generates monodisperse (the CV of diameters is below 3% for a whole generated library, and the CV of diameters is below 1% for a generated library without the last droplets generated in this library) libraries of up to *ca.* 400 droplets tested per library. We integrated the *DropChop* module into a system with a simple microdroplet dilutor based on a hydrodynamic trap,[1] and with a T-junction. We used this integrated device to generate a collection of libraries of droplets of varying and known concentrations of a sample, and we obtained this collection from a single droplet of the sample and a single droplet of a diluent infused into our device with two syringe pumps set to pump at constant rates of flow.

Known methods of splitting droplets into collections of monodisperse emulsions include splitting with a secondary stream of continuous phase: in a T-junction,[2] in a Y-junction,[3,4] in flow focusing,[5–7] and in a co-flowing stream.[8–10] Two methods of generation of relatively monodisperse emulsions without a secondary stream are 1) membrane emulsification[11] and 2) microfluidic step emulsification (MSE).[12,13] In membrane emulsification, the dispersed phase is pushed through a porous membrane. The curvature of the dispersed phase increases as the liquid passes the pore, up to a point at which the droplet breaks off.[11] A similar mechanism is employed in MSE, in which the dispersed phase traverses a small opening before entering a larger reservoir.[12,13]

In step emulsification, the dispersed phase flows through a shallow channel, traverses a step, and enters into a wide and deep channel. The part that we call 'balloon' (after Li. *et al.*;[14] the name 'tongue' has also been used for the more

Institute of Physical Chemistry, Polish Academy of Sciences, Kasprzaka 44/52, 01-224 Warsaw, Poland. E-mail: garst@ichf.edu.pl

† Electronic supplementary information (ESI) available: Dimensions of tested geometries, frequency of break-up of droplets throughout a library, recordings of emulsification of droplets at *DropChop* with bypasses, and recordings of execution of the protocol in the integrated device. See DOI: 10.1039/c7lc00014f

confined geometries[15]) of the dispersed phase that leaves the shallow channel gradually reduces its own curvature due to the expansion in the larger channel. As the curvature of the neck of the droplet phase, which is still in the narrow channel, is limited from below (*i.e.* the radius of the curvature cannot be larger than half the width or height of the channel), the Laplace pressure in the neck at some point cannot be matched by the decreasing capillary pressure in the growing balloon. The dispersed phase breaks, and the tongue in the larger channel becomes a separate droplet.[15]

Above a certain critical value of the capillary number, the step emulsification regime turns into a jetting regime, and the emulsification no longer occurs.[16] Because of that, MSE suffers from low frequencies of generation of droplets when compared to flow focusing. However, MSE can be readily parallelized for an improved frequency of generation of droplets.[17–19] Step emulsification techniques have recently gained significant attention with important new developments.[14–23]

Emulsions generated at the step are more tightly monodisperse than emulsions obtained in T-junction or flow focusing systems due to almost the same physical conditions at the step for each generated droplet.[12] However, if the step is blocked by the emulsion, the generated droplets begin to exhibit higher variation of sizes. Several solutions have been proposed to account for the problem of blocking of the step, namely, cross-flow of the continuous phase,[18–20] a sloped reservoir that uses the tendency of droplets to remain spherical,[21] buoyancy,[22] buoyancy coordinated with centrifugal forces,[17] and magnetic attraction of a ferrofluid over a step.[23]

The most commonly used microfluidic systems are oriented horizontally, and clearance of the step in such orientation is compatible only 1) with flushing of the vicinity of the step,[18–20] 2) with the sloped geometry of the reservoir that promotes escape of the generated droplets due to capillary pressure,[21] and 3) with removing ferrofluidic emulsion from the step with magnetic attraction.[23] It is generally desired to reduce the amount of external equipment in a microfluidic system, and, in this context, the sloped geometry of the reservoir is superior to the flushing and magnetic methods; still, the systems utilizing the gradient of geometry provide for limited allowed rates of flow, as the autonomous escape of droplets is rather slow.

In certain situations (such as generating libraries of small droplets presenting a serial dilution of a sample or reagent), it would be useful to first perform operations (such as dilution) on large droplets before emulsifying them into libraries. Existing solutions for step emulsification use a shallow and narrow channel that enters a larger reservoir. Large droplets in such shallow and narrow channels are long, which limits their mixing.[24,25] Additionally, the channels that could contain multiple long droplets would have to be very long themselves and produce high resistance to flow. A microfluidic solution in which a collection of large droplets of different concentrations of cells was emulsified passively was shown; however, the obtained emulsions were highly polydispersed (the range of volumes of generated droplets spread over an order of magnitude, between 2 and 16 pL) and the dilution of samples was performed outside of the microfluidic device.[26]

Our emulsification module addresses the following challenges: 1) elimination of additional pumping mechanisms for removal of generated droplets from the step and 2) rendering complex operations on large droplets before passive emulsification into monodisperse emulsions in the same microfluidic device feasible.

We integrated our emulsification module with a simple trap-based dilutor. The architecture of the trap is as we described it elsewhere.[1] Our integrated device contains a T-junction, a metering trap (dilutor), and the *DropChop* module. With this integrated device we produce a series of libraries of differing (but known) concentrations of a sample. To produce these libraries, we used two syringe pumps to perform injection of the sample and diluent at constant flow rates. We demonstrate the working principle of the integrated system using water and a dye. We present the dilution ratios of fluorescent rhodamine 110 (Sigma-Aldrich, Germany). Finally, we demonstrate emulsification of the dye at *DropChop*.

Results

The architecture of the *DropChop* module

We designed *DropChop* to passively emulsify a series of large droplets. We wanted to have a series of large droplets placed in a channel with a large cross section, so that the length of the large droplets in the series would be at most a few times larger than the width or depth of the channel to facilitate mixing inside the droplets, and also to reduce the total length of the channels in the system. Step emulsification was shown to produce droplets of diameters increasing linearly with the increasing depth of the opening above the step.[17,27,28] We aimed to produce small droplets from a collection of large droplets through step emulsification in a channel with a large cross section. We therefore reduced the depth of the channel directly before the step, so that the diameters of the droplets generated at the step would be small, but so that the large droplets approaching the step would be flowing through a large channel.

The problem arises at the transition between the large channel and the constriction. We observed that for a sudden transition from a deep (400 μm) into a shallow (70 μm) channel at a flow rate of 0.25 mL h^{-1} and at a concentration of the PFPE-PEG-PFPE fluorosurfactant[29] equal to 0.1% (w/w), a part of the droplet does not enter the constriction and thus cannot be emulsified (Fig. 1a).

To overcome the problem of a droplet not entering the constriction, we introduced a slope that leads to the constriction, and we called such geometry *DropChop*. The slope prevents the large droplet from experiencing sudden changes in its curvature when the large droplet is approaching the constriction (Fig. 1b). Without sudden changes in its curvature,

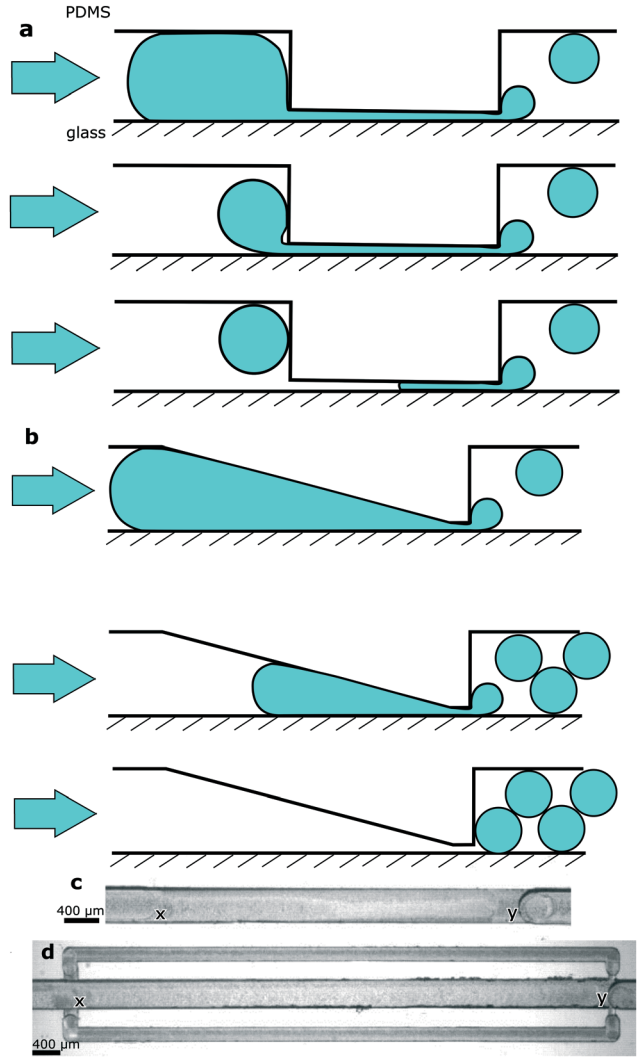

Fig. 1 a) Step emulsification of a droplet passing from a large to a small channel through a sudden transition. Part of the droplet will be locked before the transition due to unfavourable Laplace pressure and buoyancy. b) The working principle of *DropChop*. A slope in a large microchannel steadily makes the channel shallower. The slope ends in a shallow and short slit. The slit then enters a channel that has dimensions of the channel from upstream of the slope. It is possible for the whole droplet to pass the step in such a geometry. c) A micrograph of *DropChop* with a slope of 5 degrees. (*x*) The beginning of the slope. (*y*) The constriction immediately before the step. The slope in the main channel ranges between points marked with (*x*) and (*y*). d) A micrograph of *DropChop* with bypasses with a slope of 2.5 degrees. (*x*) and (*y*) are as described above.

the large droplet should be less prone to breaking before the constriction. In *DropChop*, the depth between the large channel and the constriction directly upstream of the step changes steadily. Directly downstream of the constriction, the channel becomes deeper suddenly (Fig. 1c). At this sudden transition of depths of channels, the step emulsification occurs.

In a modified version of *DropChop*, we placed two shallow channels bypassing the main channel (Fig. 1d). We put the entrance to these bypasses upstream of the slope, and we put the exit from the bypasses (into the main channel) immediately downstream of the step. The slope begins in the main channel at the location of the entrance to the bypasses.

The entrance to the bypasses is shallower and narrower than the bypasses, so that the dispersed phase does not enter the bypasses due to unfavorable Laplace pressure the droplets would have to overcome. Please consult the ESI† for the detailed dimensions of the tested devices.

DropChop (slope without bypasses)

When we emulsified large droplets at *DropChop* without the bypassing channels, the rear ends of these large mother droplets remained locked at the slope and could not pass the step. A slope of 10 degrees leading to a 70 μm high constriction locked a droplet of *ca.* 10–15 nL after emulsification of large droplets at concentrations of the fluorosurfactant equal to 0.1% (w/w) and 0.5% (w/w) at a flow rate of 0.25 mL h^{-1}. This locked droplet did not pass the step in at least 30 seconds of constant flow of the continuous phase. The mother droplet passed the slope completely when the angle of the slope was 2.5 degrees, and this complete passage occurred at a flow rate of 0.25 mL h^{-1} and at both 0.1% (w/w) and 0.5% (w/w) concentrations of the surfactant.

We therefore deemed the slope of 2.5 degrees suitable for further experiments. Increasing the flow rate led to emulsification of a whole droplet under all the mentioned conditions, although the monodispersity of emulsions obtained in such a way was decreased.

In the basic format of *DropChop* (a slope leading to a constriction, no bypassing channels), the newly formed droplets are not efficiently removed from the vicinity of the step. The droplets that stay close to the step block the formation of subsequent droplets (Fig. 2b). The formed droplets are periodically smaller and larger (Fig. 2c). This effect is especially visible in the emulsions generated at the step with a slope of 2.5 degrees, where droplets form two distinct populations of diameters (Fig. 2a and Fig. S3†).

DropChop module with bypasses for the continuous liquid

To solve the problem of generated droplets blocking the step, we introduced shallow channels that bypass the slope of the main channel. We located the entrance to the bypasses upstream of the slope, and we placed the exit from the bypasses immediately downstream of the step (Fig. 1d). When a mother droplet flows into the slope, the hydraulic resistance of the main channel increases, and a fraction of the continuous phase flows through the bypasses. The continuous phase returns to the main channel from the bypasses immediately downstream of the step, pushing the freshly generated droplets away from the vicinity of the step.

We generated libraries of droplets at a slope of 2.5 degrees with added bypasses (Fig. 1d and 3e, ESI† Movies S1 and S2) at a range of flow rates (Fig. 3a), and at a range of concentrations of the surfactant in the continuous phase (Fig. 3b). The coefficient of variance (CV) of the diameters of the generated droplets was lower than 3% at flow rates between 3 mL h^{-1}

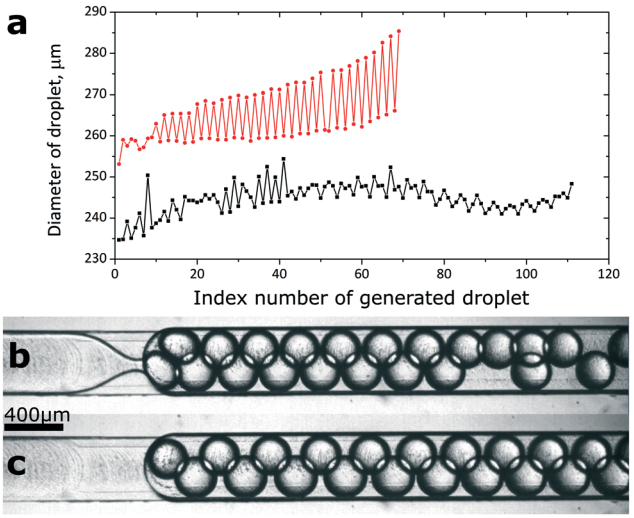

Fig. 2 a) Sizes of droplets generated at steps with slopes of 2.5 (red) and 10 (black) degrees. The droplet numbered as '1' was the first droplet generated in an emulsion. Subsequent data points are connected to emphasize the periodic changes in sizes of droplets. b) Generation of emulsion at the step with a slope of 2.5 degrees. Droplets are not removed efficiently from the point of break-up. Necking of the dispersed phase is visible in the slit. c) Rear end of the emulsion generated at the step with a slope of 2.5 degrees. Droplets in the 'bottom' row are visibly larger than the droplets in the 'top' row. The flow of fluids in (b) and (c) is realized from left to right. The scale bar applies to (b) and (c).

and 8 mL h^{-1} at 0.1% (w/w) PFPE-PEG-PFPE surfactant. The CV was higher at higher flow rates and at higher concentrations of the surfactant (Fig. 3d). Please consult the ESI† for a more detailed description of the polydispersity of emulsions generated at the highest tested concentration of the fluorosurfactant. The CV of the diameters of the first 20 droplets of an emulsion at flow rates between 2 mL h^{-1} and 12 mL h^{-1} was below 1% for all tested concentrations of the PFPE-PEG-PFPE surfactant. As for the mother droplet, the last droplet generated from this mother droplet was visibly larger or smaller than the rest of the droplets generated from it (Fig. 3a). The average diameter of the generated droplets increased slightly with the flow rate at which we performed emulsification. Increasing the flow rate by 300% (from 3 mL h^{-1} to 12 mL h^{-1}) resulted in a 5% increase in average diameter of generated droplets at 0.1% (w/w) concentration of the fluorosurfactant (Fig. 3b). The concentration of the PFPE-PEG-PFPE surfactant did not seem to affect the average diameter of the generated droplets (Fig. 3b).

Higher concentrations of the PFPE-PEG-PFPE surfactant promoted higher frequencies of generation of droplets at the tested flow rates up to 10 mL h^{-1} (Fig. 3c). At the highest tested concentration of PFPE-PEG-PFPE (1.0% <w/w>), the mother droplet would not reach the step at a flow rate of 1 mL h^{-1} and emulsification would occur at tested flow rates of 2 mL h^{-1} and higher. At lower tested concentrations of the surfactant (0.1% and 0.5% <w/w>), the mother droplet would not reach the step at tested flow rates of 1 mL h^{-1} and 2 mL h^{-1}, and emulsification would occur at tested flow rates of 3 mL h^{-1} and higher. The frequency of generation of droplets at the step rose linearly with increasing tested flow rate up to 10 mL h^{-1} at all tested concentrations of the surfactant. The frequency of generation of droplets was higher at higher concentrations of the surfactant. Moreover, the frequency of generation of droplets was not constant throughout a single library (Please consult Fig. S1 in the ESI†).

The integrated device

We integrated *DropChop* (with bypasses) with a simple microdroplet trap-based dilutor and with a simple T-junction. The order of modules downstream of the two inlet ports was as follows: T-junction, hydrodynamic trap, winding mixing channel,[30] and *DropChop* (Fig. 4a and b).

The detailed description of the hydrodynamic trap is available in our earlier work.[1] Briefly, if a droplet is larger than the volume of the trap, the trap meters a volume of the droplet that is equal to the volume of the trap. The excess volume of the droplet leaves the trap. If a droplet of the sample is locked, and a droplet of the diluent merges with this droplet of the sample, the result is a diluted droplet that is locked in the trap, and a diluted droplet that leaves the trap. We forced the coalescence of droplets inside the trap by eletrocoalescence.[32] This design of the microdroplet dilutor is similar to those of systems presented before.[1,33] Please consult the ESI† for the exact dimensions of the geometries in the integrated device.

To prepare a series of libraries of different concentrations of a sample, we used two syringe pumps with syringes filled with the continuous fluorinated phase, and connected with the device *via* PFTE tubing. We at first loaded one of the inlet tubes with a portion of the diluent, and then with a portion of the continuous phase, and finally with a portion of the sample. The other inlet tubing was filled with the fluorinated liquid. The continuous phase contained 0.1% (w/w) surfactant. We inserted the tubing into the inlet ports, and we injected the liquids into the chip using the syringe pumps at a constant flow rate of 0.03 mL h^{-1} (inlet loaded with the dispersed phase) and of 0.9 mL h^{-1} (inlet with the fluorinated phase only). The portion of the sample we loaded was similar in volume to the hydrodynamic trap. The metering trap locked the droplet of the sample. Then the T-junction divided the input droplet of the diluent into a series of smaller (*ca.* 400 nL) droplets. The series of droplets of the diluent sequentially diluted the locked droplet of the sample. Then the so generated series of droplets of decreasing concentration of the sample entered *DropChop*. *DropChop* emulsified the drops, thus generating libraries of droplets (Fig. 4f). The height of the constriction in *DropChop* in the integrated device was 30 µm. Please see the video recordings of the execution of this protocol in the ESI† (Movies S3 and S4).

In order to measure the exact ratio of dilution and assess the quality of the gradient, we employed a procedure similar to those presented before.[34–36] We carried out tests using a

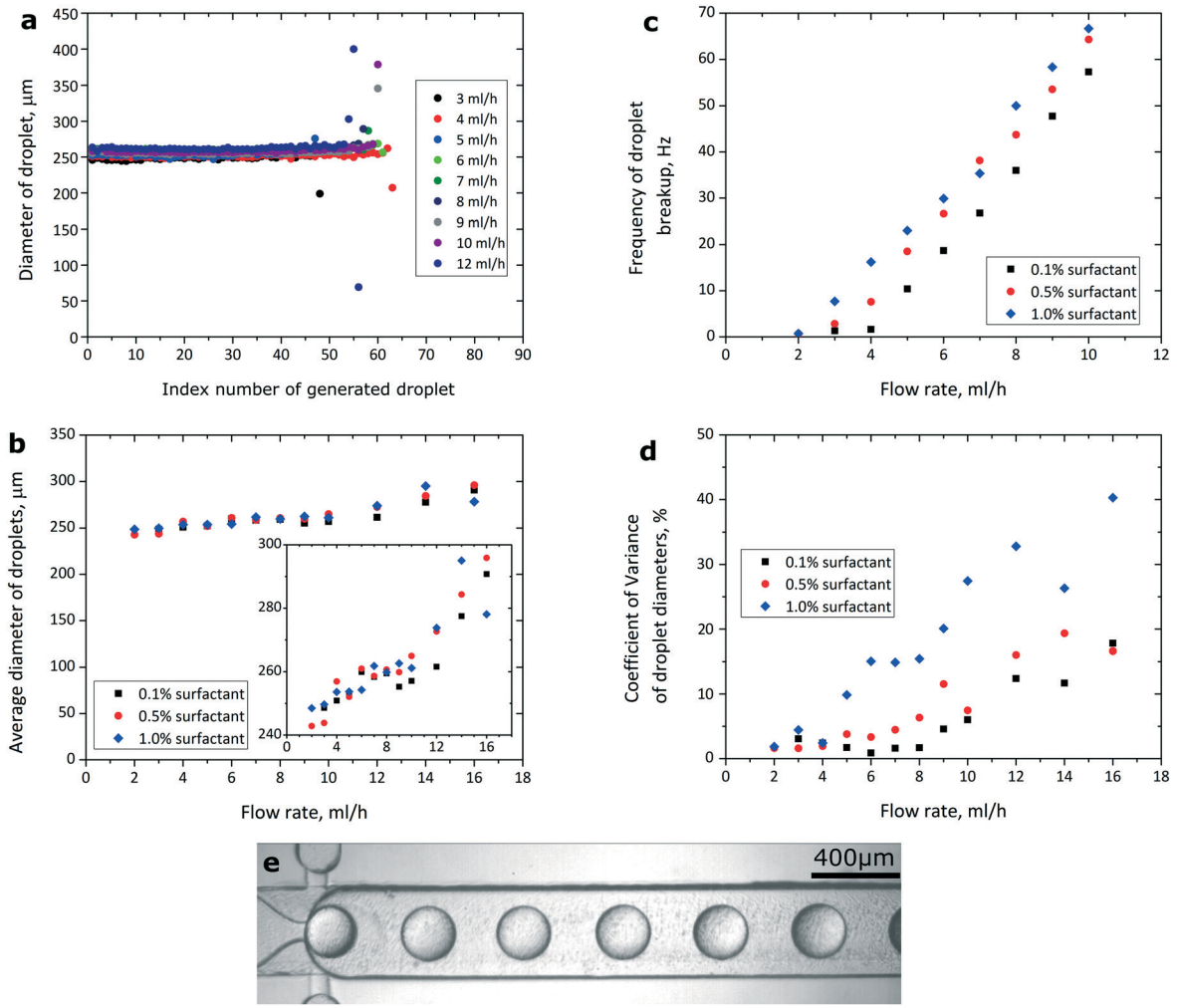

Fig. 3 a) Sizes of droplets generated at a range of flow rates and at a slope of 2.5 degrees with added bypasses (the height of the constriction before the step was 70 μm). The concentration of the fluorosurfactant was 0.1% (w/w). b) Average diameter of droplets in libraries generated at various flow rates and concentrations of the surfactant. The inset highlights that increasing the flow rate to 14 mL h^{-1} and above produces droplets with average diameters larger than what would be expected from linear dependency of droplet sizes on the flow rate at the tested flow rates up to 12 mL h^{-1}, similarly to what was shown before.[18,19] c) Frequency at which the emulsions were generated at *DropChop* at different rates of flow and at different concentrations of the fluorosurfactant in the continuous phase. The height of the slit before the step was 70 μm. d) Monodispersity of libraries generated at *DropChop* with bypasses at a range of flow rates and at a range of concentrations of the fluorosurfactant. e) Droplets generated at a step with added bypasses. The flow rate was 5 mL h^{-1}, and the concentration of the surfactant was 1.0% (w/w). Droplets do not interfere with each other, providing for increased monodispersity when compared with the geometry without bypasses.

50 μM solution of rhodamine 110 in water with an addition of methanol (0.1% w/w) as a sample. For the diluent, we used pure water. We measured the mean intensity of fluorescence of every droplet. The measured parts of droplets were the same in size in two subsequent droplets and were localized centrally in every droplet. We then calculated the ratio of the intensities of fluorescence between consecutive droplets, and we defined this value as the ratio of dilution. For each pair of subsequent droplets, we adjusted the sensitivity of the detector of fluorescence to adapt the dynamic range of the measurement system to the concentration of rhodamine in a given pair of droplets. We set the sensitivity of the detector so that the brighter droplet (with a higher concentration of rhodamine 110) had an intensity of fluorescence of *ca.* 3000 arbitrary units (a.u.) in the NIS-Elements software (Nikon, Japan) that we use to operate our confocal microscope, which is well below the threshold of saturation (at 4095 a.u.).

The average dilution ratio obtained from 20 dilutions was 1.37 with a coefficient of variance of 6.1% (Fig. 4c).

We generated 8 droplets each of *ca.* 400 nL at a T-junction, and after the dilution protocol, we emulsified these droplets at *DropChop*. We obtained 8 libraries of droplets, and the libraries contained an average of 392 ± 9 droplets with an average diameter of 120 μm (*ca.* 900 pL). The coefficient of variance of the diameters of all generated droplets (total: 3134 droplets) was *ca.* 4%. We defined outlying droplets as those of diameters smaller than 115 μm (*ca.* 800 pL). Outlying droplets were generated always as the last droplets of each library (Fig. 4e). Without the outlying droplets of each library, the coefficient of variance of the diameters was below

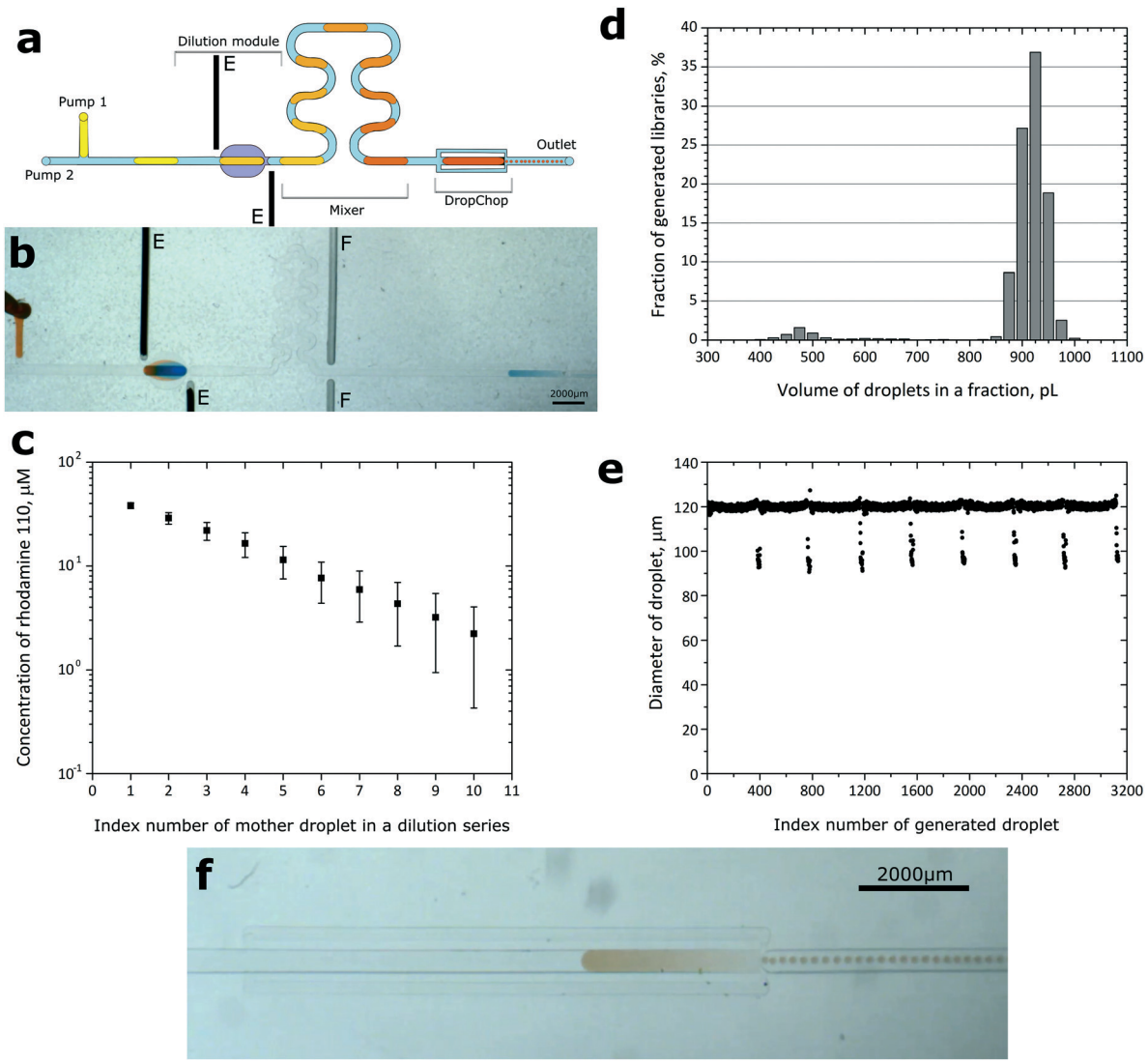

Fig. 4 a) Schematics of *DropChop* with bypasses integrated with a trap-based dilutor. A series of droplets of the diluent would dilute a sample locked in the trap, and then the diluted series of droplets after passing a mixing channel would be passively emulsified at *DropChop*. The electrodes (*E*) located close to the dilutor force the electrocoalescence of drops. b) Execution of the protocol. Dilution of the sample occurs in the dilution module. Emulsification occurs at *DropChop*. '*F*' marks channels initially meant for a 'Faraday moat',[31] but those channels were not used and were empty during the experiments. c) Rate of dilution between subsequent droplets generated at the T-junction in our integrated device. The points on the graph are a result of averaging of two measurements. Error bars are calculated from the accumulating error (coefficient of variance of measured dilution ratios) of dilution. d) Distribution of obtained volumes of droplets in emulsions generated at *DropChop*, calculated from 8 mother droplets and 3134 daughter droplets. e) Diameters of 3134 droplets in libraries generated from 8 mother droplets, presented in order of generation. The average diameter of generated droplets was 120 μm. The coefficient of variance of the diameters was *ca.* 4%, and without the outlying droplets the CV of the diameters was below 1%. f) Emulsification of a large droplet of dye at *DropChop*.

1% for all measured libraries. 5% of the droplets in each library (18 ± 2 per library) was outlying. The average diameter of the outlying droplets was 98 μm (the CV of the diameters of only outlying droplets equaled 4.4%), which corresponds to *ca.* 490 pL. The majority of the outlying droplets were of a diameter of 92–98 μm (volume of *ca.* 400–500 pL) (Fig. 4d).

Discussion

The parameters of the emulsions generated at *DropChop* depend on the geometry of the channels. The high angle of the slope stops the rear end of a drop from passing the step, leaving a droplet locked at the slope, *via* a mechanism similar to that described earlier.[37] A small marauding droplet leaves more space for gutters of the continuous phase when compared to a large, elongated droplet at a slope. The continuous phase preferably flows around the locked droplet through the gutters, rather than pushing the droplet over the step. The differences in behavior of the rear-end droplet at various angles of the slope stem from the fact that a droplet is more spherical at a steeper slope than at a more gentle slope. It is more energetically unfavorable for a drop to pass the narrow

opening over the step after a steep slope than after a gentler slope.

We showed that droplets generated at a step after a slope without bypasses form subpopulations of diameters. This is because the already generated droplets block the formation of the subsequent droplets. Periodicity is less visible at higher angles of the slope. This might be because more time might be needed for a droplet to be separated from the bulk water phase at a steep slope when compared to a gentle slope due to different values of Laplace pressure inside droplets at slopes of different angles. During this longer break-up, a higher amount of the continuous phase would pass the step per single generated droplet. The higher amount of the continuous phase would push the generated droplet farther away from the step than in the case of a gentler slope, thus reducing the effect of obstruction of new droplets.

The addition of the bypassing channels around the main sloped channel allowed for efficient removal of the generated droplets from the area immediately after the step. The removal of freshly generated droplets from the vicinity of the step ensured no obstructions after the step, and thus generation of monodisperse emulsions at *DropChop* with bypasses was possible. The images of the process of emulsification show a neck forming in the dispersed phase, and the profile of the distribution of volumes of droplets in a library compared to profiles obtained at a flow-focusing device by Kaminski *et al.*[7] suggests that the mechanism of break-up at *DropChop* with bypasses is step emulsification, rather than flow-focusing. The droplets are generated at the step, and then the continuous phase that flows from the bypasses pushes the droplets away from the step.

The average diameter of the generated droplets changed only slightly over a range of flow rates. This might be partially due to the fact that a fraction of the flowing continuous phase runs through the bypasses, and thus this fraction does not increase the speed of the droplet at the step. *DropChop* with bypasses required higher flow rates than *DropChop* without bypasses to operate properly. Additionally, *DropChop* (with bypasses) with a smaller height of the slit required a higher rate of flow to ensure emulsification than *DropChop* with a larger height of the slit. This is a result of 1) increased hydraulic resistance of the main channel with a slit of decreased height, which leads to the continuous phase flowing preferably through the bypasses and 2) increased Laplace pressure in a droplet traversing a slit of decreased height. The diameters of the generated droplets seem not to depend (or seem to depend only weakly) on the concentration of the surfactant.

Higher tested concentrations of the surfactant 1) enabled emulsification at lower flow rates and 2) increased the frequency of generation of droplets at a given flow rate. This might be connected with the Laplace pressure present in the droplet at the slope. We forced a droplet into a steadily narrowing channel, so the curvature of the droplet at the front of this droplet was steadily increasing. Increasing curvature means increasing Laplace pressure that is forcing the droplet back from the narrowing channel. At a critical point, at which the pressure generated by the syringe pumps on the droplet is matched by the Laplace back-pressure, the droplet becomes locked at the slope.[37] By increasing the concentration of the surfactant (this generally decreases the value of surface tension), we reduced this Laplace back-pressure. At a lower Laplace back-pressure, the droplet reached the step at a lower flow rate (lower forward pressure). The increased frequency of generation of droplets at higher concentrations of surfactant is in agreement with predictions and experiments.[14,23] Similarly, the linear dependency of the frequency of generation of droplets on the flow rate is in concert with predictions and experiments shown earlier.[14,17,18,38]

As any step-based emulsifier, *DropChop* does not emulsify properly (*i.e.* in the step emulsification regime) at high values of capillary number in the system. It would be useful to alleviate this problem, because some biochemical assays, like PCR, use reagent mixtures that would probably have a lower value of surface tension in comparison with what we have tested. A modification of *DropChop* that would reliably emulsify such a reagent mixture would open a way to exploit *DropChop* in droplet digital PCR (ddPCR) assays.[4,17,39,40] Possibly an increase in the angle of the slope combined with bypasses of cross sections larger than we tested would help, since these modifications would reduce the speed of the droplet at the step.

The microfluidic systems we present here may also be used for applications in synthetic and materials chemistry, as our geometries are capable of producing highly monodispersed droplets, even at less precise control of the rate of flow. For instance, one of the most promising applications of droplet microfluidics is the synthesis of nanocrystals and nanoparticles.[41–43] However, the devices that we used in this study were made of PDMS, which is not a suitable material to operate with a wide range of organic solvents[44] commonly used in synthetic chemistry. Nevertheless, our geometries might be fabricated in other more chemically resistant materials, such as Teflon[45] or polycarbonate with surface modification compatible with fluorinated oil and, at the same time, resistant to the most commonly used organic solvents.[46]

DropChop could benefit from shorter bypasses and a shorter slope, for the sake of miniaturization. In the integrated device, we used a slope that was *ca.* 8 mm long at a 2.5 degree incline. Perhaps a shorter slope of *e.g.* 10 degrees that changes the angle to 2.5 degrees not long upstream of the step would be operating in a manner comparable to the system we presented here.

Conclusions

Here we showed a microfluidic geometry capable of generating emulsions of monodisperse droplets without sources of pressure dedicated to clearing the vicinity of the step. A sloped geometry upstream of the step, in combination with bypassing channels around the slope, allows for the generation of monodisperse emulsions from multiple large

droplets. We showed that our geometry is of a modular character, and we integrated this geometry with a trap-based droplet dilutor. We generated a collection of libraries of monodisperse sub-nanoliter droplets of varying but known concentrations of a sample. We achieved this with only two syringe pumps that were simply set to run at constant rates of flow.

Our work might be of interest to those willing to reduce the number of syringe pumps in their microfluidic systems. Passive generation of libraries of varying and known concentrations of a sample might be used in digital-based analytical schemes.

DropChop is a system that allows for truly passive emulsification of large droplets in microfluidic channels. It can be used to perform complex microfluidic assays with a reduced amount of external equipment.

DropChop does not perform emulsification properly at high values of capillary number. This limits the capability of *DropChop* in assays that use reagent mixtures that have very low values of surface tension. Overcoming this issue would open *DropChop* for assays such as ddPCR, and a collection of libraries of droplets of different concentrations of a target nucleic acid would fit the existing algorithms for ddPCR.[47]

Materials and methods

Fluids

We used Novec HFE7500 (3M, USA) as the continuous phase in all described experiments. The PFPE-PEG-PFPE fluorosurfactant was synthesized according to the protocol described by Holtze *et al.*[29]

Fabrication of the devices

To fabricate the devices, we first produced polycarbonate molds using a CNC milling machine (MSG4025, Ergwind, Poland). We then poured PDMS (Sylgard 184, Dow Corning, USA) onto the polycarbonate mold and we polymerized PDMS at 70 °C for 2 hours. We then treated the PDMS mold for 3 h under 10 mbar pressure with vapors of tridecafluoro-1,1,2,2,-tetrahydrooctyl)-1-trichlorosilane (United Chemical Technologies, USA). We then used the negative molds to cast PDMS positive chips. We bonded the PDMS chips with glass slides (1 mm thick) by treating PDMS chips and glass slides with plasma and placing them together. We rendered the microfluidic channels hydrophobic by filling the chip with Novec 1720 (3M, USA). When the fluid evaporated from the channels at room temperature, we baked the chip at 135 °C for 15 minutes.

Electric field

We used an electric field to facilitate the coalescence of droplets in the trap-based dilutor in the integrated device. The electric field was alternating at 200 Hz at 1.5 kV. The electrodes were no further than 4 mm from each other.

Acknowledgements

The project was co-financed by the European Research Council Starting Grant 279647 and by the National Science Centre through the Symfonia Grant (DEC2014/12/W/NZ6/00454). T. S. K. was supported by the Ministry of Science and Higher Education through the scholarship for outstanding young researchers (0722/E-64/STYP/10/295). This project was partially performed in the laboratories funded by NanoFun POIG.02.02.00-00-025/09.

References

1 P. M. Korczyk, L. Derzsi, S. Jakieła and P. Garstecki, *Lab Chip*, 2013, **13**, 4096–4102.
2 D. R. Link, S. L. Anna, D. A. Weitz and H. A. Stone, *Phys. Rev. Lett.*, 2004, **92**, 054503.
3 A. R. Abate and D. A. Weitz, *Lab Chip*, 2011, **11**, 1911–1915.
4 A. C. Hatch, J. S. Fisher, A. R. Tovar, A. T. Hsieh, R. Lin, S. L. Pentoney, D. L. Yang and A. P. Lee, *Lab Chip*, 2011, **11**, 3838–3845.
5 A. B. Theberge, E. Mayot, A. El Harrak, F. Kleinschmidt, W. T. S. Huck and A. D. Griffiths, *Lab Chip*, 2012, **12**, 1320–1326.
6 A. R. Abate, T. Hung, R. A. Sperling, P. Mary, A. Rotem, J. J. Agresti, M. A. Weiner and D. A. Weitz, *Lab Chip*, 2013, **13**, 4864–4869.
7 T. S. Kaminski, S. Jakiela, M. A. Czekalska, W. Postek and P. Garstecki, *Lab Chip*, 2012, **12**, 3995–4002.
8 H. Lee, C.-H. Choi, A. Abbaspourrad, C. Wesner, M. Caggioni, T. Zhu, S. Nawar and D. A. Weitz, *Adv. Mater.*, 2016, **38**, 8425–8430.
9 C.-X. Zhao, D. Chen, Y. Hui, D. A. Weitz and A. P. J. Middelberg, *ChemPhysChem*, 2016, **17**, 1553–1556.
10 C.-H. Choi, H. Lee, A. Abbaspourrad, J. H. Kim, J. Fan, M. Caggioni, C. Wesner, T. Zhu and D. A. Weitz, *Adv. Mater.*, 2016, **28**, 3340–3344.
11 S. M. Joscelyne and G. Trägårdh, *J. Membr. Sci.*, 2000, **169**, 107–117.
12 S. Sugiura, M. Nakajima and M. Seki, *Langmuir*, 2002, **18**, 3854–3859.
13 T. Kawakatsu, Y. Kikuchi and M. Nakajima, *J. Am. Oil Chem. Soc.*, 1997, **74**, 317–321.
14 Z. Li, A. M. Leshansky, L. M. Pismen and P. Tabeling, *Lab Chip*, 2015, **15**, 1023–1031.
15 R. Dangla, E. Fradet, Y. Lopez and C. N. Baroud, *J. Phys. D: Appl. Phys.*, 2013, **46**, 114003.
16 M. Hein, J.-B. Fleury and R. Seemann, *Soft Matter*, 2015, **11**, 5246–5252.
17 F. Schuler, F. Schwemmer, M. Trotter, S. Wadle, R. Zengerle, F. von Stetten and N. Paust, *Lab Chip*, 2015, **15**, 2759–2766.
18 N. Mittal, C. Cohen, J. Bibette and N. Bremond, *Phys. Fluids*, 2014, **26**, 082109.

19 K. van Dijke, G. Veldhuis, K. Schroën and R. Boom, *Lab Chip*, 2009, **9**, 2824–2830.
20 E. Amstad, M. Chemama, M. Eggersdorfer, L. R. Arriaga, M. P. Brenner and D. A. Weitz, *Lab Chip*, 2016, **16**, 4163–4172.
21 R. Dangla, S. C. Kayi and C. N. Baroud, *Proc. Natl. Acad. Sci. U. S. A.*, 2013, **110**, 853–858.
22 F. Dutka, A. S. Opalski and P. Garstecki, *Lab Chip*, 2016, **16**, 2044–2049.
23 S. Kahkeshani and D. Di Carlo, *Lab Chip*, 2016, **16**, 2474–2480.
24 K. Handique and M. A. Burns, *J. Micromech. Microeng.*, 2001, **11**, 548–554.
25 J. D. Tice, H. Song, A. D. Lyon and R. F. Ismagilov, *Langmuir*, 2003, **19**, 9127–9133.
26 E. Um, S.-G. Lee and J.-K. Park, *Appl. Phys. Lett.*, 2010, **97**, 153703.
27 L. Shui, A. van den Berg and J. C. T. Eijkel, *Microfluid. Nanofluid.*, 2011, **11**, 87–92.
28 S. Sugiura, M. Nakajima, S. Iwamoto and M. Seki, *Langmuir*, 2001, **17**, 5562–5566.
29 C. Holtze, A. C. Rowat, J. J. Agresti, J. B. Hutchison, F. E. Angilè, C. H. J. Schmitz, S. Köster, H. Duan, K. J. Humphry, R. A. Scanga, J. S. Johnson, D. Pisignano and D. A. Weitz, *Lab Chip*, 2008, **8**, 1632–1639.
30 H. Song, J. D. Tice and R. F. Ismagilov, *Angew. Chem., Int. Ed.*, 2003, **42**, 768–772.
31 B. O'Donovan, T. Tran, A. Sciambi and A. Abate, *J. Visualized Exp.*, 2014, **86**, e50913.
32 K. Ahn, J. Agresti, H. Chong, M. Marquez and D. A. Weitz, *Appl. Phys. Lett.*, 2006, **88**, 264105.
33 X. Niu, F. Gielen, J. B. Edel and A. J. deMello, *Nat. Chem.*, 2011, **3**, 437–442.
34 J. Fan, B. Li, S. Xing and T. Pan, *Lab Chip*, 2015, **15**, 2670–2679.
35 B. M. Paegel, W. H. Grover, A. M. Skelley, R. A. Mathies and G. F. Joyce, *Anal. Chem.*, 2006, **78**, 7522–7527.
36 S. Ahrar, M. Hwang, P. N. Duncan and E. E. Hui, *Analyst*, 2014, **139**, 187–190.
37 M. G. Simon, R. Lin, J. S. Fisher and A. P. Lee, *Biomicrofluidics*, 2012, **6**, 014110.
38 C. Priest, S. Herminghaus and R. Seemann, *Appl. Phys. Lett.*, 2006, **88**, 024106.
39 B. J. Hindson, K. D. Ness, D. A. Masquelier, P. Belgrader, N. J. Heredia, A. J. Makarewicz, I. J. Bright, M. Y. Lucero, A. L. Hiddessen, T. C. Legler, T. K. Kitano, M. R. Hodel, J. F. Petersen, P. W. Wyatt, E. R. Steenblock, P. H. Shah, L. J. Bousse, C. B. Troup, J. C. Mellen, D. K. Wittmann, N. G. Erndt, T. H. Cauley, R. T. Koehler, A. P. So, S. Dube, K. A. Rose, L. Montesclaros, S. Wang, D. P. Stumbo, S. P. Hodges, S. Romine, F. P. Milanovich, H. E. White, J. F. Regan, G. A. Karlin-Neumann, C. M. Hindson, S. Saxonov and B. W. Colston, *Anal. Chem.*, 2011, **83**, 8604–8610.
40 C. M. Hindson, J. R. Chevillet, H. A. Briggs, E. N. Gallichotte, I. K. Ruf, B. J. Hindson, R. L. Vessella and M. Tewari, *Nat. Methods*, 2013, **10**, 1003–1005.
41 I. Shestopalov, J. D. Tice and R. F. Ismagilov, *Lab Chip*, 2004, **4**, 316–321.
42 A. M. Nightingale, T. W. Phillips, J. H. Bannock and J. C. de Mello, *Nat. Commun.*, 2014, **5**, 3777.
43 T. W. Phillips, I. G. Lignos, R. M. Maceiczyk, A. J. de Mello and J. C. de Mello, *Lab Chip*, 2014, **14**, 3172–3180.
44 J. N. Lee, C. Park and G. M. Whitesides, *Anal. Chem.*, 2003, **75**, 6544–6554.
45 K. Ren, W. Dai, J. Zhou and H. Wu, *Proc. Natl. Acad. Sci. U. S. A.*, 2011, **108**, 8162–8166.
46 P. Jankowski, D. Ogonczyk, W. Lisowski and P. Garstecki, *Lab Chip*, 2012, **12**, 2580–2584.
47 P. R. Debski, K. Gewartowski, M. Sulima, T. S. Kaminski and P. Garstecki, *Anal. Chem.*, 2015, **87**, 8203–8209.